

Direct neutron capture cross section on ^{80}Ge and probing shape coexistence in neutron-rich nuclei

S. Ahn,^{1,2,3,4,*} D. W. Bardayan,^{2,5} K. L. Jones,¹ A. S. Adekola,⁶ G. Arbanas,⁷
J. C. Blackmon,⁸ K. Y. Chae,⁹ K. A. Chipps,^{10,1} J. A. Cizewski,⁶ S. Hardy,⁶ M. E. Howard,^{6,11}
R. L. Kozub,¹¹ B. Manning,⁶ M. Matoš,⁸ C. D. Nesaraja,² P. D. O'Malley,^{6,5} S. D. Pain,²
W. A. Peters,¹² S. T. Pittman,^{1,8} B. C. Rasco,⁸ M. S. Smith,² and I. Spassova¹²
¹*Department of Physics and Astronomy, University of Tennessee, Knoxville, Tennessee 37996, USA*
²*Physics Division, Oak Ridge National Laboratory, Oak Ridge, Tennessee 37831, USA*
³*Joint Institute for Nuclear Astrophysics, Michigan State University, East Lansing, Michigan 48824, USA*
⁴*National Superconducting Cyclotron Laboratory, Michigan State University, East Lansing, Michigan 48824, USA*
⁵*Department of Physics, University of Notre Dame, Notre Dame, IN 46556, USA*
⁶*Department of Physics and Astronomy, Rutgers University, New Brunswick, New Jersey 08903, USA*
⁷*Reactor and Nuclear Systems Division, Oak Ridge National Laboratory, Oak Ridge, Tennessee 37831, USA*
⁸*Department of Physics and Astronomy, Louisiana State University, Baton Rouge, Louisiana 70803, USA*
⁹*Department of Physics, Sungkyunkwan University, Suwon 16419, South Korea*
¹⁰*Department of Physics, Colorado School of Mines, Golden, Colorado 80401, USA*
¹¹*Department of Physics, Tennessee Technological University, Cookeville, Tennessee 38505, USA*
¹²*Oak Ridge Associated Universities, Oak Ridge, Tennessee 37830, USA*
(Dated: August 30, 2019)

Results are presented from the first neutron-transfer measurement on ^{80}Ge using an exotic beam from the Holifield Radioactive Ion Beam Facility at Oak Ridge National Laboratory. Newly-measured spins and spectroscopic factors of low-lying states of ^{81}Ge are determined, and the neutron-capture cross section on ^{80}Ge was calculated in a direct-semi-direct model to provide a more realistic (n,γ) reaction rate for r -process simulations. Furthermore, a region of shape coexistence around $N \sim 50$ is confirmed and implications for the magic nature of ^{78}Ni are discussed.

The rapid neutron capture process (r -process) occurs in astrophysical environments with exceedingly high temperatures (> 1 GK) and neutron densities ($> 10^{22}/\text{cm}^3$), and is the source of roughly half of the elements heavier than iron [1]. Recent gravitational wave observations have provided evidence that one r -process site is neutron star mergers [2]. Observations of metal-poor halo stars provide a detailed picture of the robustness of the main r -process abundance pattern [3], but currently our knowledge of the nuclear physics of exotic neutron-rich nuclei, especially of lighter elements related to the astrophysical site of the weak r -process, lags behind.

During r -process freeze-out, the temperature drops and the $(n,\gamma) - (\gamma,n)$ equilibrium breaks. Neutron capture reactions on abundant nuclei can significantly alter the number of free neutrons, affecting the final abundances of hundreds of nuclei [4, 5]. Sensitivity studies [6] demonstrated that this effect at the $A = 80$ peak in the solar abundance pattern occurs on select nuclei around neutron closed shells, including ^{80}Ge . The $^{80}\text{Ge}(n,\gamma)$ rate was shown to have a significant impact on final abundances with more than twice the impact of either the $^{82}\text{Ge}(n,\gamma)$ or $^{84}\text{Se}(n,\gamma)$ reaction rates where the direct-semi-direct (DSD) capture has been calculated based on measured properties [7]. It has not been possible to estimate the direct (n,γ) rate on ^{80}Ge with any level of con-

fidence because the spin assignments and spectroscopic strengths of low-lying ^{81}Ge levels were unknown.

Understanding the spectroscopic properties of low-lying intruder states in ^{81}Ge also provides an important gauge of shape coexistence in this region of the nuclear chart. For mid-shell nuclei, it is well known that the spherical nuclear shell model fails to reproduce observed excitation energies and residual interactions such as particle correlations. Collective motions, or deformations, of nuclei must also be considered to explain shape coexistence, as attempted by many different theoretical models [8–14]. The changes in nuclear structure can be studied along isotopic or isotonic chains of one particle or hole with respect to the closed shell. An increase in excitation energy of intruder states along an isotopic or isotonic chain, for example, is an indicator that a shell closure is being approached.

The Ge isotopes represent an excellent example of rapid shape changes along an isotopic chain. Near stability, ^{72}Ge exhibits shape coexistence [15], whereas ^{74}Ge , ^{76}Ge , and ^{78}Ge have triaxial natures [16–19]. Beyond the $N = 50$ shell closure, the more neutron-rich Ge isotopes, $^{84,86,88}\text{Ge}$, are proposed to resume triaxiality based upon their low-lying level schemes [20]. A recent study of ^{80}Ge [21] observed an intruder 0^+ state below the first 2^+ , unlike the vast majority of even-even nuclei where the first excited state is the 2^+_1 level, and making a strong case for shape coexistence.

A limited number of investigations of neutron-rich nuclei one neutron above, or one neutron below $N = 50$ via direct reactions have been reported e.g. [7, 22], as

* Present Address: Cyclotron Institute, Texas A&M University, College Station, Texas, 77843, USA

beams of rare ions at sufficient intensities for reaction measurements have become available. There have also been β decay and laser spectroscopy measurements of these $N = 49$ nuclei [23, 24]. In this manuscript, the first transfer-reaction study of low-lying intruder states in ^{81}Ge is described. The goal was to determine spectroscopic factors for pertinent ^{81}Ge levels, leading to the first calculation of DSD neutron-capture on ^{80}Ge that relies upon measured, instead of estimated, level parameters. Additionally, this study provides clarification of shape coexistence occurring in ^{81}Ge .

The only previous study of low-lying levels in ^{81}Ge inferred level properties from the observations of γ rays following the β decay of ^{81}Ga and the β -delayed neutron decay of ^{82}Ga [25]. Precise level energies for low-lying ^{81}Ge levels were obtained, but spins were estimated. Evidence was found for a low-lying isomeric state with $J^\pi = \frac{1}{2}^+$, contrary to the $\frac{1}{2}^-$ spin found for isomers in other odd-mass $N = 49$ isotones. While this inversion was explained as a possible sign of shape coexistence in the level systematics study [25], a transfer reaction study on ^{82}Se [26], and theoretical work on the odd-mass $N = 49$ isotones [11], it was impossible to make any definitive confirmation of the exotic phenomena with the tentative spin assignments and unknown spectroscopic factors of the observed states. Because the first excited state in ^{80}Ge is $J^\pi = 0^+$, in contrast to the $J^\pi = 2^+$ first excited state in ^{82}Se , it is not appropriate to simply assume the same spectroscopic properties for excited states in ^{81}Ge as the $N = 49$ isotone ^{83}Se .

To address these uncertainties, the $^{80}\text{Ge}(d,p)^{81}\text{Ge}$ reaction was measured in inverse kinematics at the Holifield Radioactive Ion Beam Facility (HRIBF) [27] at Oak Ridge National Laboratory. Similar to the study of $^{82}\text{Ge}(d,p)^{83}\text{Ge}$ [7], a strong population of low-lying single-particle $\frac{1}{2}^+$ and $\frac{5}{2}^+$ states was expected with only weak (or no) population of the $\frac{1}{2}^-$ hole state. The spectrum of populated states, along with angular distributions of emitted protons, enables constraints to be placed on the spin assignments of these levels.

A ^{80}Ge beam [28, 29] at 310 MeV (3.875 MeV/u) bombarded a $174 \mu\text{g}/\text{cm}^2$ -thick $(\text{CD}_2)_n$ target for 5 days. A fast ionization counter (IC) [30] was placed downstream of the target chamber to detect and identify the beam components and the ^{81}Ge recoils. The beam was $\sim 98\%$ pure, and an average rate of $\sim 10^5$ pps was obtained. In addition, a stable ^{80}Se beam was provided for internal energy and angle calibrations of the silicon detectors using the well-known states of ^{81}Se [31].

The energies and angles of light-ion ejectiles from the (d,d) and (d,p) reactions were measured by various silicon detectors (one Micron S1 [32] covering $\theta_{lab} = 154^\circ - 170^\circ$, one SIDAR [33] for $\theta_{lab} = 124^\circ - 154^\circ$, one Micron X3 [34] for $\theta_{lab} = 50^\circ - 89^\circ$, two Micron SX3s [35] for $\theta_{lab} = 50^\circ - 124^\circ$, and one Micron BB15 [36] for $\theta_{lab} = 50^\circ - 124^\circ$). Polar angular resolutions were typically less than 2 degrees.

A charged-particle energy spectrum of events in coincidence with a germanium ion being detected in the IC is shown in Fig. 1. The upper proton bands of the (d,p) re-

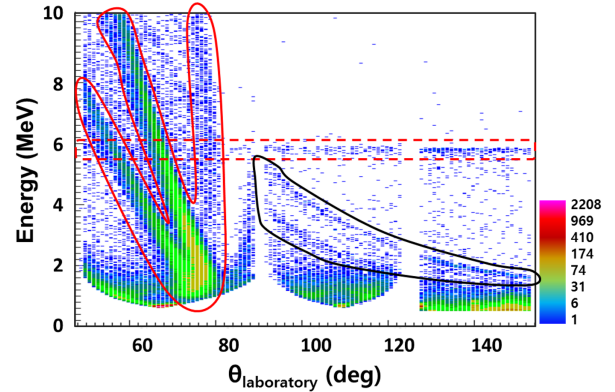


FIG. 1. (color online). A spectrum of detected particle energy vs. laboratory angle gated on a time coincidence with a forward going recoil detected in the IC. Detected protons, deuterons, and carbon ions (surrounded by the red solid line) are from elastic scattering. Protons from the (d,p) reaction are in the region marked by the black line. The horizontal band at 5.8 MeV (in the dashed red rectangle) arises from a ^{244}Cm calibration source.

action in the spectrum are evident at $Q = 1.94 \pm 0.05$ MeV and 1.48 ± 0.07 MeV with a full-width half-maximum resolution of 0.26 MeV as shown in Fig. 2. The corresponding energies of levels in ^{81}Ge are $E_x = 0.69 \pm 0.05$ MeV and 1.16 ± 0.07 MeV, respectively. Since this experiment was designed to probe the spin of the $E_x = 679$ keV level, discussion in the remainder of this manuscript is limited to the strongly populated peak at $E_x = 0.69 \pm 0.05$ MeV. This peak is consistent with the population of levels previously observed at $E_x = 679$ keV and 711 keV and not consistent with the population of other known ^{81}Ge levels [25, 31]. No evidence was observed for population of a level at $E_x = 896$ keV, which is consistent with the inference made in Ref. [25] that this level is tentatively a $\frac{1}{2}^-$ hole state. The $\frac{9}{2}^+$ ground state is also not populated, as expected as an $\ell = 4$ angular momentum transfer is unfavorable in a (d,p) reaction at this beam energy.

The spin assignments of observed states could be constrained from the angular distributions of protons emitted from the reaction compared to calculations using the adiabatic wave approximation including finite range effects (ADWA-FR) [37, 38], shown in Fig. 3. The data were binned in angular ranges ($\Delta\theta_{c.m.} \approx 2^\circ$ for SIDAR and 4° for Micron SX3 and BB15) to increase the statistical precision of the individual data points in the distributions. The plotted error bars in Fig. 3 are statistical in nature. The ADWA-FR calculations use nucleonic (instead of nuclear) potentials and explicitly include deuteron breakup [39]. The deuteron adiabatic potential was constructed using the Johnson and Tandy optical parameterization method [38] with Chapel-Hill 89 (CH89) [40] nucleonic potentials for the neutron and

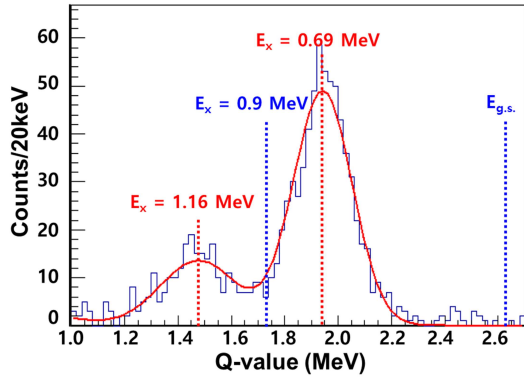


FIG. 2. (color online). Q -value spectrum of protons in coincidence with a germanium recoil from the $^{80}\text{Ge}(d,p)^{81}\text{Ge}$ reaction, detected in the SIDAR and Micron SX3 detectors. Considering 0.05-MeV FWHM energy resolution of one state from the energy calibration using $^{80}\text{Se}(d,p)^{81}\text{Se}$ reactions and the precise level energies of ^{81}Ge from Ref. [25], two states are expected to be populated in the peak at $E_x = 0.69$ MeV with 0.25-MeV FWHM resolution. The ground-state Q -value of the reaction is $Q = 2.63$ MeV.

the proton. The CH89 global optical potential was also used for the exit channel. All transfer calculations in this work were performed with FRESKO [41], and adiabatic potentials were obtained with a modified version of TWOFNR [42]. Fixed standard radius and diffuseness parameters, $r_0 = 1.25$ fm and $a = 0.65$ fm, respectively, were used for the bound state. The Reid interaction [43] was used to obtain the deuteron wave function and the transfer operator.

The differential cross-sections in Fig. 3 favor calculations that include s-wave transfers (red curve) rather than the one including p-wave transfers (dark green curve). Since it is well known [44–46] that the calculated transfer cross-sections better represent the data on the first peak of the angular distribution, spectroscopic factors were obtained by fitting the most-forward angle data only. The shape of the red curve in Fig. 3 shows the best fit using this procedure.

The angular distributions were also analyzed using a Distorted Wave Born Approximation (DWBA) analysis (not shown here) in order to compare with ADWA-FR. In this case, global (Lohr-Haeblerli [47] + CH89) optical potentials were used for the entrance and exit channels. Note that DWBA does not take into account deuteron breakup. The fit of $\ell = 0$ and $\ell = 2$ angular momentum transfer mixing in the calculation gave the best result with the data, similar to the ADWA-FR results. We, therefore, conclude that the 679-keV level is a $\frac{1}{2}^+$ state with a strong $3s_{\frac{1}{2}}$ component and the state at 711 keV is $\frac{5}{2}^+$ with a strong $2d_{\frac{5}{2}}$ component, consistent with previous work. The β -decay study [25] deduced the $t_{1/2}$ of the 679-keV isomer and found that it was consistent with $J^\pi = \frac{1}{2}^+$ and that the spin-parity of the 711-keV state was consistent with $\frac{5}{2}^+$. In addition, the observation of

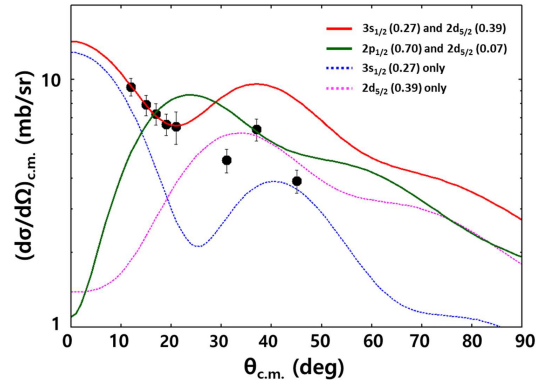


FIG. 3. (color online). Proton angular distributions in the center of mass from backward-angle detectors compared to differential cross sections calculated with FRESKO [41] for the unresolved doublet at $E_x = 679$ and 711 keV. For the red curve, $3s_{\frac{1}{2}}$ transfer was assumed for the 679-keV state (dash blue) and $2d_{\frac{5}{2}}$ transfer to the 711-keV component (dash magenta). For the dark green curve, $2p_{\frac{1}{2}}$ transfer was assumed for the 679-keV state. The first five data points at the most forward angles are used to fit the curves. In parentheses after the shell model configuration are the spectroscopic factors that result from the fit of the theoretical to experimental differential cross sections.

an apparent shift in centroid as a function of angle, from $E_x = 670 \pm 50$ keV to $E_x = 700 \pm 50$ keV, supports our conclusion of an unresolved doublet.

Spectroscopic factors were extracted from the angular distributions considering the single peak results from the population of two levels ($\frac{1}{2}^+$ and $\frac{5}{2}^+$) shown in Table I. The quoted uncertainties are the combination in quadrature of the statistical best-fit uncertainty (30%), the estimated uncertainty in the target thickness (13%), the systematic uncertainty (10%) due to the geometrical parameters in the detector setup, and the theoretical uncertainty (25%) from a sensitivity study of the calculation. This last uncertainty was estimated by varying the bound-state potential radius, r , between 1.25 to 1.35 fm and examining the effect on the spectroscopic factors.

The present result, supported by precise level energies for low-lying ^{81}Ge levels from Ref. [25], consistently shows that the spins and parities of the states at $E_x = 679$ keV and 711 keV in ^{81}Ge are $\frac{1}{2}^+$ and $\frac{5}{2}^+$ with significant $3s_{\frac{1}{2}}$ and $2d_{\frac{5}{2}}$ components, respectively. The ground state of ^{81}Ge has one hole in the neutron closed shell at $N = 50$ and four valence protons above the proton closed shell $Z = 28$. The ground state is expected to be a neutron single-hole state in the $1g_{\frac{7}{2}}$ orbital, while positive parity excited states are from the population of levels above the $N = 50$ closed shell. Since the energy of the $N = 50$ shell gap for Ge isotopes was measured to be $\Delta = S_{2n}(^{82}\text{Ge}) - S_{2n}(^{84}\text{Ge}) = 3.15$ MeV [48], the energies of the 679 and 711-keV states are very low compared to the shell gap, and thus a naive shell model picture is

TABLE I. Spectroscopic factors deduced from ADWA-FR calculations of low-lying intruder states in ^{81}Ge from the measurements of the $^{80}\text{Ge}(d,p)^{81}\text{Ge}$ neutron transfer reaction in inverse kinematics.

$E_x(\text{keV})$	J^π	S_{nlj}
679	$\frac{1}{2}^+$	$S_{3s\frac{1}{2}} = 0.27 \pm 0.11$
711	$\frac{5}{2}^+$	$S_{2d\frac{5}{2}} = 0.39 \pm 0.17$

not adequate. The observation of $3s_{\frac{1}{2}}$ and $2d_{\frac{5}{2}}$ strength at low excitation energies is a signature of intruder states that can be described as neutron 1p-2h configurations.

As shown in Fig. 4, the same type of intruder states were found in the odd-mass $N = 49$ isotones ^{83}Se [26, 49], ^{85}Kr [50] and ^{87}Sr [51]. It is interesting to note that the levels in ^{81}Ge are slightly shifted up from those in ^{83}Se , which is the pivot point of the trend line. This is consistent with ^{83}Se being near the middle of the $Z = 28 \sim 40$ subshell. Furthermore, this result suggests that the intruder states of $N = 49$ isotones are expected to continue to rise in energy approaching doubly-magic ^{78}Ni . A recent study on ^{79}Zn ($Z = 30$) [22] supports this hypothesis.

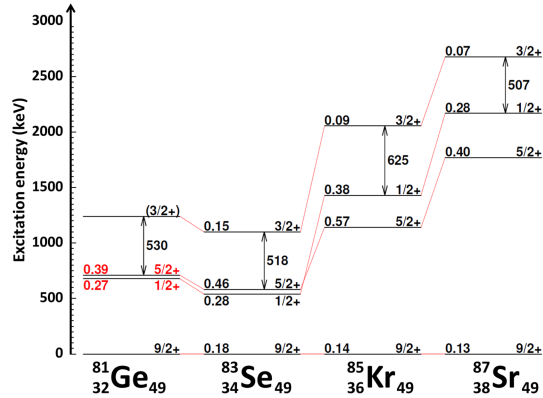


FIG. 4. (color online). Intruder states ($J^\pi = \frac{1}{2}^+$, $\frac{5}{2}^+$ and $\frac{3}{2}^+$) of the even $Z < 40$, $N = 49$ isotones. Spectroscopic factors extracted from transfer reactions (numbers on the left edge of the level) are also shown as well as spin and parity (right edge of the level). Data for ^{81}Ge are from the present work (red numbers) and Ref. [25]. Data for the other odd-mass $N = 49$ isotones: ^{87}Sr from Ref. [51], ^{85}Kr from Ref. [50] and ^{83}Se from Ref. [26].

As mentioned above, the astrophysical $^{80}\text{Ge}(n,\gamma)^{81}\text{Ge}$ reaction rate is important for the final abundances in the r-process, particularly in the $A \sim 80$ peak. The spins and positive parities of the first two states of ^{81}Ge , measured in the present work, mean that the dominant direct capture contributions are expected to be through either s-wave or d-wave neutron capture with a magnetic dipole (M1) transition or p-wave neutron capture with an electric dipole (E1) transition [52]. In addition to direct capture, the giant dipole resonance (GDR) effect can

be accounted for via semi-direct capture [53]. The neutron capture cross-section was computed in a DSD model with the code CUPIDO [53]. Optimized parameters from a similar study of $^{82}\text{Ge}(n,\gamma)^{83}\text{Ge}$ [7] were adopted in the present calculations. We assumed that p-wave neutrons are captured on ^{80}Ge via an E1 transition into the lowest 3s and 2d single-particle states of ^{81}Ge . The difference between the DSD capture and the direct capture is smaller than 10%. The total cross-section, displayed in Fig. 5, was calculated as a sum of individual cross sections, weighted by the spectroscopic factors deduced in this work.

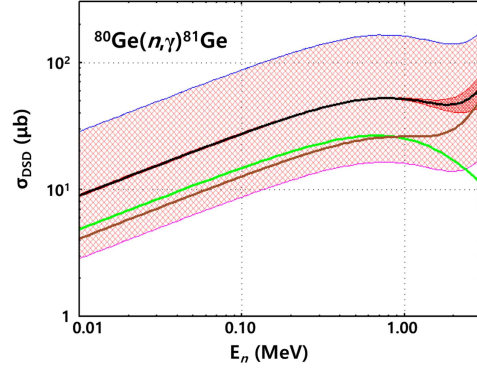


FIG. 5. (color online). Calculated DSD cross sections (black curve) for the $^{80}\text{Ge}(n,\gamma)^{81}\text{Ge}$ reaction. Individual contributions are also plotted with the green curve for the $3s_{\frac{1}{2}}$ orbital and the brown curve for the $2d_{\frac{5}{2}}$ orbital. The lower limit of the red hashed band shows the calculation with $S_{3s\frac{1}{2}} = 0.16$ and $S_{2d\frac{5}{2}} = 0.56$, and the upper limit was calculated with $S_{3s\frac{1}{2}} = 0.38$ and $S_{2d\frac{5}{2}} = 0.22$. A dashed light red band represents calculated cross sections for the $E_x = 679$ keV case with spectroscopic factor $S_{nlj} = 1$ (top, blue) and 0.1 (bottom, purple). The uncertainty of the cross section is $\sim 30\%$, similar to the uncertainties in the spectroscopic factors extracted here.

To highlight the impact of our present measurements, we calculated the DSD cross section with spectroscopic factors ranging from 0.1 to 1 as an estimate of the uncertainty in the cross section prior to the present study. Note that the uncertainty of neutron capture rates from this variation is much less than the range of the sensitivity study performed in Ref. [6], which was a factor of 100. As seen in Fig. 5, the unconstrained DSD capture cross section can vary by nearly an order of magnitude. Our measurement has reduced this uncertainty by more than a factor of 20.

In summary, the $^{80}\text{Ge}(d,p)^{81}\text{Ge}$ transfer reaction has been studied at the HRIBF with an exotic ^{80}Ge beam to enhance our understanding of low-lying levels in ^{81}Ge ($N = 49$) that are important to nucleosynthesis. The tentative spins and parities of the first and second excited states were validated and the spectroscopic factors of the states were extracted from our data using the ADWA-FR formalism. The spins of the states are consistent with a previous β -decay measurement of ^{81}Ga and calculations

from a unified theory model, expanding our knowledge of shape coexistence to exotic nuclei. Additional measurements of the spin-parities and spectroscopic factors of the intruder levels in ^{77}Ni are important to confirm these conclusions. Using these experimental results, the DSD capture cross sections for the $^{80}\text{Ge}(n,\gamma)^{81}\text{Ge}$ have been calculated, and the uncertainties are reduced by more than a factor of 20. This new result provides a more realistic (n,γ) cross section needed for r-process nucleosynthesis simulations.

Note that neutron capture on ^{80}Ge via formation of a compound nucleus (CN) followed by statistical decay could be significantly larger than the DSD process we have calculated, as seen in ^{82}Se isotone study [54]. However, predicting such processes on a weakly bound nucleus near a shell closure, such as ^{80}Ge is highly uncertain. To inform the CN (n,γ) cross section on ^{80}Ge would require a validated surrogate [55] for neutron capture on radioactive ion beams, as was recently demonstrated for the $(d,p\gamma)$ reaction [56, 57].

The authors are grateful to J. M. Allmond,

J. L. Wood and R. K. Grzywacz for very useful discussions. This work is supported in part by the U.S. Department of Energy, Office of Science, Office of Nuclear Physics under contract numbers DE-FG02-96ER40983 (UT), DE-SC0001174(UT), DE-FG02-96ER40955 (TTU), DE-AC05-00OR22725 (ORNL), DE-FG02-96ER40978 (LSU), the U.S. Department of Energy, National Nuclear Security Administration Stewardship Science Academic Alliance Program under contracts DE-FG52-08NA28552 and DE-NA0002132 (Rutgers), through the US Department of Energy Topical Collaboration TORUS and by the National Science Foundation under grant PHY-1067806 (Rutgers) and grant PHY-1419765 (Notre Dame) and a National Research Foundation of Korea (NRF) grant funded by the Korea government Ministry of Education, Science, and Technology (MEST) Nos. NRF-2014S1A2A2028636, NRF-2015R1D1A1A01056918, NRF-2016K1A3A7A09005579, and NRF-2016R1A5A1013277. This research was conducted at the Oak Ridge National Laboratory Holifield Radioactive Ion Beam Facility, a former D.O.E. Office of Science User Facility.

-
- [1] E. M. Burbidge, G. R. Burbidge, W. A. Fowler, and F. Hoyle, *Rev. Mod. Phys.* **29**, 547 (1957).
 - [2] N. R. Tanvir *et al.*, *Ap. J. Lett.* **848**, L27 (2017).
 - [3] C. Sneden, J. J. Cowan, and R. Gallino, *Annu. Rev. Astron. Astrophys.* **46**, 241 (2008).
 - [4] J. Beun, J. C. Blackmon, W. R. Hix, G. C. McLaughlin, M. S. Smith, and R. Surman, *J. Phys. G* **36**, 025201 (2009).
 - [5] R. Surman, J. Beun, G. C. McLaughlin, and W. R. Hix, *Phys. Rev. C* **79**, 045809 (2009).
 - [6] R. Surman, M. Mumpower, R. Sinclair, K. L. Jones, W. R. Hix, and G. C. McLaughlin, *AIP Advances* **4**, 041008 (2014).
 - [7] J. S. Thomas *et al.*, *Phys. Rev. C* **76**, 044302 (2007).
 - [8] K. Heyde, *The Nuclear Shell Model*, Springer, Berlin, 1994.
 - [9] S. L. Heller, and J. N. Friedman, *Phys. Rev. C* **10**, 1509 (1974).
 - [10] K. Heyde, M. Waroquier, and R. A. Meyer, *Phys. Rev. C* **17**, 1219 (1978).
 - [11] R. A. Meyer, O. G. Lien, III, and E. A. Henry, *Phys. Rev. C* **25**, 682 (1982).
 - [12] K. Heyde, P. Van Isacker, M. Waroquier, J. L. Wood, and R. A. Meyer, *Phys. Rep.* **102**, 291 (1983).
 - [13] J. L. Wood, K. Heyde, W. Nazarewicz, M. Huyse, and P. van Duppen, *Phys. Rep.* **215**, 101 (1992).
 - [14] K. Heyde, and J. L. Wood, *Rev. of Mod. Phys.* **83**, 1467 (2011).
 - [15] H. T. Fortune, *Phys. Rev. C* **94**, 024318 (2016).
 - [16] J. J. Sun *et al.*, *Phys. Lett. B* **734**, 308 (2014).
 - [17] Y. Toh *et al.*, *Phys. Rev. C* **87**, 041304(R) (2013).
 - [18] S. Mukhopadhyay *et al.*, *Phys. Rev. C* **95**, 014327 (2017).
 - [19] A. M. Forney *et al.*, *Phys. Rev. Lett.* **120**, 212501 (2018).
 - [20] M. Lettmann *et al.*, *Phys. Rev. C* **96**, 011301 (2017).
 - [21] A. Gottardo *et al.*, *Phys. Rev. Lett.* **116**, 182501 (2016).
 - [22] R. Orlandi *et al.*, *Phys. Lett. B* **740**, 298 (2015).
 - [23] A. Korgul *et al.*, *Phys. Rev. C* **86**, 024307 (2012).
 - [24] X. F. Yang *et al.*, *Phys. Rev. Lett.* **116**, 182502 (2016).
 - [25] P. Hoff and B. Fogelberg, *Nucl. Phys.* **A368**, 210 (1981).
 - [26] L. A. Montestrucque *et al.*, *Nucl. Phys.* **A305**, 29 (1978).
 - [27] J. R. Beene *et al.*, *J. Phys. G* **38**, 024002 (2011).
 - [28] D. W. Stracener, *Nucl. Instr. and Meth. B* **204**, 42 (2003).
 - [29] D. W. Stracener *et al.*, *Nucl. Instr. and Meth. A* **521**, 126 (2004).
 - [30] K. Y. Chae *et al.*, *Nucl. Instr. and Meth. A* **751**, 6 (2014).
 - [31] C. M. Baglin, *Nucl. Data Sheets* **109**, 2257 (2008).
 - [32] <http://www.micronsemiconductor.co.uk/silicon-detector-catalog>
 - [33] D. W. Bardayan *et al.*, *Phys. Rev. C* **63**, 065802 (2001).
 - [34] S. D. Pain *et al.*, *Nucl. Instr. and Meth. B*, **261**, 1122 (2007).
 - [35] E. Koshchiy *et al.*, *Nucl. Instr. and Meth. A* **870**, 1 (2017).
 - [36] D. W. Bardayan *et al.*, *Nucl. Instr. and Meth. A* **711**, 160 (2013).
 - [37] R. C. Johnson, and P. J. R. Soper, *Phys. Rev. C* **1**, 976 (1970).
 - [38] R. C. Johnson, and P. C. Tandy, *Nucl. Phys.* **A235**, 56 (1974).
 - [39] F. M. Nunes, and A. Deluva, *Phys. Rev. C* **84**, 034607 (2011).
 - [40] R. L. Varner, W. J. Thompson, T. L. McAbee, E. J. Ludwig, and T. B. Clegg, *Phys. Rep.* **201**, 57 (1991).
 - [41] I. J. Thompson, *Comput. Phys. Rep.* **7**, 167 (1988).
 - [42] M. T. J. Tostevin, M. Igarashi, and N. Kishida, *University of Surrey modified version of the code TWOFNR* (private communication).
 - [43] R. V. Reid, *Ann. Phys.* **50**, 411 (1968).
 - [44] J. P. Schiffer *et al.*, *Phys. Rev.* **164**, 1274 (1967).
 - [45] D. Y. Pang *et al.*, *Phys. Rev. C* **75**, 024601 (2007).

-
- [46] I. J. Thompson, and F. M. Nunes, *Nuclear Reactions for Astrophysics: Principles, Calculation and Applications of Low-Energy Reactions*, Cambridge University Press, 2009.
- [47] J.M. Lohr and W. Haeberli, *Nucl. Phys.* **A232**, 381 (1974).
- [48] J. Hakala *et al.*, *Phys. Rev. Lett.* **101**, 052502 (2008).
- [49] E. K. Lin, *Phys. Rev.* **139**, B340 (1965).
- [50] N. A. Detorje, P. L. Jolivet, C. P. Browne, and A. A. Rollefson, *Phys. Rev. C* **18**, 991 (1978).
- [51] B. L. Burks, R. E. Anderson, T. B. Clegg, E. J. Ludwig, B. C. Karp and Y. Aoki, *Nucl. Phys. A* **457**, 337 (1986).
- [52] T. Rauscher, R. Bieber, H. Oberhummer, K.-L. Kratz, J. Dobaczewski, P. Möller, and M. M. Sharma, *Phys. Rev. C* **57**, 2031 1998.
- [53] W. E. Parker *et al.*, *Phys. Rev. C* **52**, 252 (1995).
- [54] M. Herman and A. Marcinkowski, *Nucl. Phys. A* **357**, 1 (1981).
- [55] J. E. Escher *et al.*, *Rev. Mod. Phys.* **84**, 353 (2012).
- [56] A. Ratkiewicz *et al.*, *Phys. Rev. Lett.* **122**, 052502 (2019).
- [57] S.D. Pain *et al.*, *Physics Procedia*, **90**, 455 (2017).